NASA TECHNICAL MEMORANDUM

NASA TM X-3552

PERIMENTAL PERFORMANCE OF 16.10-CENTIMETER-TIP-DIAMETER EPTBACK CENTRIFUGAL COMPRESSOR SIGNED FOR A 6:1 PRESSURE RATIO

gh A. Klassen, Jerry R. Wood,
d Lawrence F. Schumann

ois Research Center

ois Directorate,
. Army Air Mobility R&D Laboratory
veland, Ohio 44135

IONAL AERONAUTICS AND SPACE ADMINISTRATION · WASHINGTON, D. C. · JUNE 1977

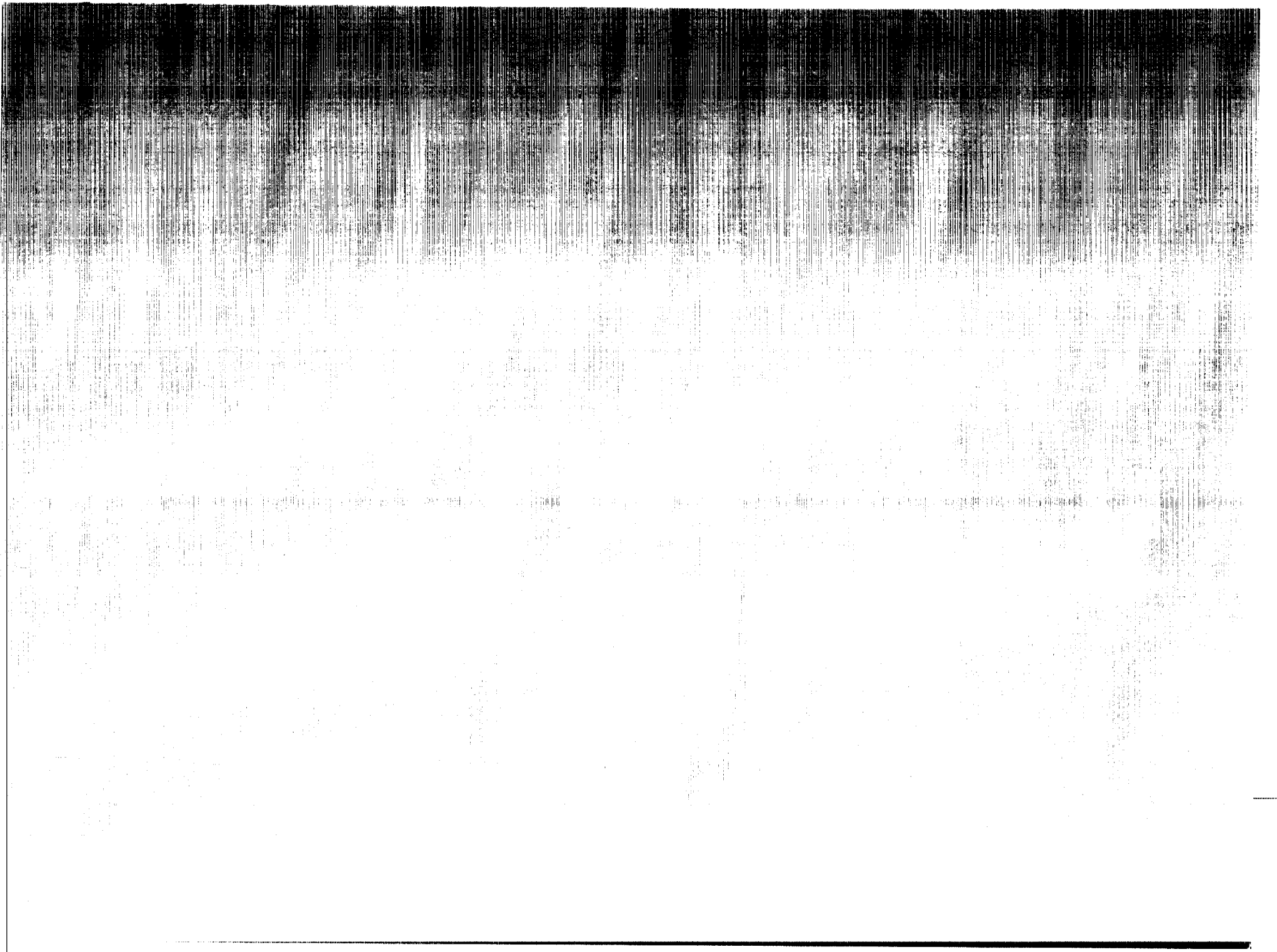

1. Report No. NASA TM X-3552	2. Government Accession No.	3. Recipient's Catalog No.
4. Title and Subtitle EXPERIMENTAL PERFORMANCE OF A 16.10-CENTIMETER-TIP-DIAMETER SWEPTBACK CENTRIFUGAL COMPRESSOR DESIGNED FOR A 6:1 PRESSURE RATIO		5. Report Date June 1977 6. Performing Organization Code
7. Author(s) Hugh A. Klassen, Jerry R. Wood, and Lawrence F. Schumann		8. Performing Organization Report No. E-9074 10. Work Unit No. 505-04
9. Performing Organization Name and Address NASA Lewis Research Center and U.S. Army Air Mobility R&D Laboratory Cleveland, Ohio 44135		11. Contract or Grant No. 13. Type of Report and Period Covered Technical Memorandum
12. Sponsoring Agency Name and Address National Aeronautics and Space Administration Washington, D.C. 20546		14. Sponsoring Agency Code

15. Supplementary Notes

16. Abstract

Tests of a backswept impeller with design mass flow rate of 1.033 kg/sec were conducted with both a vaned diffuser and a vaneless diffuser to establish stage and impeller characteristics. Design stage pressure ratio of 5.9:1 was attained at a flow slightly lower than the design value. Flow range at design speed was 6 percent of choking flow. Impeller axial tip clearance at design speed was varied to determine effect on stage and impeller performance.

17. Key Words (Suggested by Author(s))	18. Distribution Statement		
Compressor Centrifugal compressor	Unclassified - unlimited STAR Category 02		
19. Security Classif. (of this report) Unclassified	20. Security Classif. (of this page) Unclassified	21. No. of Pages 30	22. Price* A03

* For sale by the National Technical Information Service, Springfield, Virginia 22161

EXPERIMENTAL PERFORMANCE OF A 16.10-CENTIMETER-TIP-DIAMETER SWEPTBACK CENTRIFUGAL COMPRESSOR DESIGNED FOR A 6:1 PRESSURE RATIO

by Hugh A. Klassen, Jerry R. Wood, and Lawrence F. Schumann

Lewis Research Center and
U. S. Army Air Mobility R&D Laboratory

SUMMARY

The performance of a 16.1-centimeter-tip-diameter centrifugal compressor with 34^{o} of backsweep was investigated to establish baseline performance for single stage centrifugal compressors with approximately 6:1 pressure ratio and approximately 1-kilogram-per-second corrected mass flow rate. The compressor was designed for a total pressure ratio of 5.9:1 at an equivalent mass flow rate of 1.033 kilogram per second and an equivalent speed of 68 384 rpm. Overall performance with a vane-island diffuser was determined for four different design speed axial tip clearances. Impeller performance over the entire impeller operating range was determined by replacing the vane-island diffuser with a vaneless diffuser. The impeller was tested at four different design speed axial tip clearances.

For an impeller axial tip clearance of 6.4 percent of exit blade height, peak overall total efficiency at design aerodynamic speed was 0.778. Peak total pressure ratio was 6.13. Flow range between choke and surge decreased from 16 to 6 percent of choking flow as equivalent speed was increased from 90 to 100 percent of design. Equivalent mass flow rate at design pressure ratio is 1.8 percent below design. Overall peak efficiency is reduced by about 0.24 points for each 1 percent increase in impeller axial clearance at 100 percent speed. Peak efficiency was 0.796 at 90 percent speed for 3.9 percent design speed axial tip clearance.

For the tests with the vaneless diffuser, peak impeller efficiency at design speed increased from 0.866 to 0.895 and pressure ratio increased as axial tip clearance was decreased from 9.6 to 3.7 percent. At an equivalent mass flow rate of 0.972 kilogram per second, the impeller pressure ratio increased from 6.7 to 7.2.

When the ratio of mass flow at choke to design mass flow divided by the fractional speed is plotted versus percent speed, the component limiting flow is easily determined. This method shows that stage choke is controlled by the diffuser below 95 percent speed and by the inducer above 95 percent speed.

INTRODUCTION

In recent years, there has been a renewed interest in the use of centrifugal compressors in gas turbine engines for small engine applications such as helicopters, auxiliary power units (APU), general aviation, surface vehicles, and so forth as well as for the last stage of large core engines. This interest results from initial cost savings, ruggedness and high single stage pressure ratios attainable with centrifugal compressors. As a result of this interest, the Lewis Research Center has initiated a program to investigate single stage centrifugal compressors designed for pressure ratios between six and ten and equivalent mass flow rates of approximately 1 kilogram per second. The program is intended to establish baseline performance for current single stage compressors and to evaluate advanced concepts that have the potential to improve stage efficiency and surge to choke flow range. Concepts such as tandem inducer and diffuser blading, boundary layer bleed, vortex generators, variable area diffusers and partial admission may be considered.

As part of this program a conventional compressor with a backswept impeller and a vane-island diffuser was experimentally evaluated. The design equivalent mass flow is 1.033 kilograms per second and the design overall pressure ratio is 5.9:1. Design equivalent speed is 68 384 rpm. The impeller is a modified version of one supplied to the Air Force in an APU. It is considered to be representative of current technology. The impeller and diffuser are described in reference 1. Impeller flow range and performance characteristics were obtained by replacing the vane-island diffuser with a vaneless diffuser. The vaneless diffuser allows the impeller to operate over its entire operating range and together with the overall performance gives indications of impeller-diffuser matching problems. Both sets of tests were made at four design speed impeller exit axial tip clearances to establish the effect of clearance on overall performance as well as impeller performance for this type of compressor.

This report presents the performance characteristics obtained for this centrifugal compressor. Overall performance is shown with curves of total efficiency and total pressure ratio as functions of equivalent mass flow and design speed axial tip clearance with lines of constant equivalent speed. Impeller performance with a vaneless diffuser is shown with curves of total efficiency and total pressure ratio as functions of equivalent mass flow and axial tip clearance at design speed only.

COMPRESSOR AERODYNAMIC DESIGN

Overall design operating characteristics are the following:

Equivalent mass flow rate, $w\sqrt{\theta}/\delta$, kg/sec	1.033
Total pressure ratio, P'_3/P'_0	5.91
Equivalent speed, $N/\sqrt{\theta}$, rpm	68 384
Specific speed, N_s, $\omega\sqrt{Q_0}/\Delta h'^{3/4}_{id}$	0.718
Total efficiency, η_{0-3}	0.778

(Symbols are defined in appendix A.)

Compressor Flow Passage

Figure 1 shows a meridional view of the compressor flow passage. Impeller exit flow is reduced from a Mach number of 1.11 to 0.855 by a vaneless space before entering the vane-island diffuser. A second vaneless space downstream from the diffuser provides additional velocity reduction to a Mach number of 0.173.

Impeller

A photograph of the impeller is shown in figure 2. Design velocity diagrams inside the blade row are shown in figure 3. Blade coordinates are given in reference 1. Design geometry and performance characteristics are:

Number of blades	19
Inlet tip diameter, cm	10.01
Inlet hub/tip ratio	0.433
Exit blade height, cm	0.516
Exit tip diameter, cm	16.10
Design axial tip clearance/exit blade height	0.039
Total pressure ratio, P'_2/P'_0	6.95
Total efficiency, η_{0-2}	0.871

Impeller efficiency and pressure ratio are calculated inside the impeller assuming no aerodynamic blockage but accounting for blade blockage.

Diffuser

Figure 4 is a drawing of the vane-island diffuser blades as well as the design inlet and exit velocity diagrams. Reference 1 contains additional details. Design geometry and performance characteristics are as follows:

Characteristic	Vaneless space 1	Vane-island diffuser	Vaneless space 2
Radius ratio, exit/inlet	1.16	1.34	1.27
Inlet Mach number	1.11	.855	.226
Exit Mach number	.855	.226	.173
Compressor total pressure ratio at exit	6.56	5.93	5.91
Compressor total efficiency at exit	.837	.780	.778

Efficiency values are for constant values of specific heat ratio ($\gamma = 1.4$). Use of variable thermodynamic properties in calculating efficiency would give a compressor efficiency of 0.769 at the second vaneless space. For the vaneless diffuser test the vaneless diffuser had a passage height of 0.536 centimeter which is the same as for the vaned diffuser. The vaneless diffuser had a sudden expansion to twice passage height at a radius 123 percent of the impeller exit radius.

Deviations from Design

Inspection of the impeller revealed several geometrical discrepancies between design and actual hardware. Figures 5 and 6 show comparisons of measured hardware and design intent. Figure 5 shows that the actual inlet blade angle β_b was fabricated as per the design intent. The leading edge normal thickness is nearly twice as large as the design value near the tip and appears to be nearly equal to the design value in the hub part of the blade. A simple calculation of design and actual inducer inlet area showed that there was a 3 percent reduction in area due to the increased blade thickness. Figure 6 shows the exit blade angle β_b is 2° to 3.5° lower than the design value. Exit normal thickness is about twice as large as the design value.

APPARATUS, INSTRUMENTATION, AND PROCEDURE

Test Facility

Figure 7 shows a schematic of the compressor test facility. The compressor and turbine are on a common shaft. Compressor mass flow rate was measured with a choked flow nozzle on the inlet line and with the calibrated bellmouth on the compressor inlet. Compressor inlet pressure was automatically controlled by a valve on the inlet line to the plenum chamber. Compressor discharge pressure was manually controlled with a remotely operated valve in the compressor discharge line. Drive turbine speed was automatically controlled by a valve on the turbine inlet line. A hydrogen combustor was used to provide turbine inlet temperatures up to approximately 480 K. Turbine discharge pressure was manually controlled by two remotely operated valves in the turbine discharge line.

Instrumentation

The compressor instrument stations are shown in figure 8. The compressor inlet instrumentation is located in the plenum chamber and consists of two combination total temperature-total pressure probes spaced 90° apart. Each probe measures four total pressure samples and two total temperature samples. The bellmouth was instrumented with three static taps located in the throat. The discharge measuring station (station 3) is located in the second vaneless space downstream of the diffuser vanes (fig. 1) where the design Mach number is 0.173. This station consists of three total pressure probes and three shielded total temperature probes. Static pressures were measured along the impeller shroud and along the diffuser to the discharge measuring station. At impeller exit (station 2), static pressure was obtained from the average of six static taps spanning one diffuser pitch. For the impeller performance tests with the vaneless diffuser, static pressures were measured along the shroud and in the vaneless space. Instrumentation at the discharge measuring station was the same as for the vaned diffuser tests.

Procedure

All tests were run with air at a compressor total temperature of approximately 292 K. Inlet total pressure was approximately 9.9 N/cm^2. Impeller exit to shroud axial clearance was varied by shimming the shroud away from the impeller. The diffuser position was not changed so that the first vaneless space passage height increased as the clearance increased. For each shim thickness, data were obtained at 50, 60, 70, 80, 90, and 100 percent of design equivalent speed. All clearance values discussed in this

report are referenced to design equivalent speed. At design speed, overall compressor performance was obtained at axial tip clearance values of 3.9, 6.4, 8.9, and 11.3 percent of exit blade height. For the vaneless diffuser tests, clearances at design speed were 3.7, 5.7, 7.9, and 9.6 percent. Rub probes with graphite tips were used to measure clearance. Clearance as a function of speed was determined by measuring the change in probe length resulting from the graphite being worn away by the impeller. Mass flow rates were varied from choke to surge. At the smallest clearances for both the vaned and vaneless diffuser tests, the compressor was not surged. This was to avoid a possible rub caused by increased impeller deflection at surge. The compressor work used to compute overall efficiency was obtained from the actual enthalpy increase across the impeller. Total enthalpies at the compressor inlet and exit were obtained from the measured total temperatures at stations 0 and 3 using tables of gas properties.

Impeller total efficiencies and pressure ratios were calculated from measured total temperatures assuming constant specific heat ($\gamma = 1.4$) and no aerodynamic blockage at the impeller exit, since only trends were desired. The exit blade speed U was obtained from the measured rotative speed. The exit tangential velocity V_u was obtained from the relation: $UV_u = \Delta h'$. The remainder of the velocity diagram was constructed from continuity using the measured equivalent mass flow, the static pressure at impeller exit and no aerodynamic blockage. The resulting calculated total pressure was used to calculate impeller efficiency and pressure ratio. In order to obtain absolute values of impeller efficiency and pressure ratio, detailed knowledge of actual flow conditions at the impeller exit would be required.

RESULTS AND DISCUSSION

Tests were conducted on a conventional backswept 6:1 pressure ratio, 1.033 kilograms per second mass flow centrifugal compressor in order to determine baseline performance. The test results are presented in three sections. In the first section, the variation of impeller tip clearance with speed is discussed. In the second section, overall compressor performance with the vane-island diffuser is shown over a range of equivalent speeds and axial tip clearances. In the third section, impeller characteristics are shown for design equivalent speed only. These were obtained by replacing the vane-island diffuser with a vaneless diffuser. This allowed testing of the impeller over its entire flow range. Recirculation losses at the impeller exit associated with circumferential pressure gradients caused by stagnation of the flow on the leading edge of the diffuser vanes were eliminated by this substitution. A comparison of recirculation losses estimated by the method given in reference 2 is made.

Variation of Impeller Tip Clearance With Speed

Clearance decreased continually with increasing speed between zero and 100 percent design equivalent speed. The change in percent clearance with speed is shown in figure 9. The base point of zero at 100 percent speed has been selected so that the percent clearance at any speed can be determined by adding any value on the curve to the design speed percent clearance value.

Overall Compressor Performance

Design speed compressor performance with a vaned diffuser was obtained at design speed axial tip clearance values of 3.9, 6.4, 8.9, and 11.3 percent of impeller exit blade height. For each design speed clearance setting, performance was also obtained over a range of equivalent speed from 50 to 90 percent of design in increments of 10 percent without any change in shim size. Overall compressor efficiency is shown in figure 10 as a function of equivalent mass flow and axial tip clearance. The tip clearance figures given in the figure are those obtained at design speed only. The curves for 8.9 percent clearance are not shown because efficiencies for 8.9 and 11.3 percent clearances were essentially the same. This figure shows that as clearance decreases, efficiency improves at all speeds.

A peak efficiency of 0.796 was attained at 90 percent speed for the 3.9 percent design speed clearance. At any given design speed clearance the efficiency improves as speed is increased from 60 to 90 percent of design speed. This is due in part to the decreasing axial clearance as speed is increased (see fig. 9) and improved matching of impeller and diffuser characteristics. A drop of 1.1 points in peak efficiency occurs as speed is increased from 90 to 100 percent speed. An explanation for this decrease may be seen in figure 11 where impeller efficiency η_{0-2} and diffuser total pressure loss coefficient $\bar{\omega}_{2-3}$ are plotted against mass flow rate. At 80 percent design speed peak impeller efficiency occurs at a mass flow rate (0.705 kg/sec) which is greater than the mass flow rate (0.62 kg/sec) at which minimum diffuser total pressure loss occurs. At 90 percent of design speed, peak impeller efficiency and minimum diffuser total pressure loss occurs almost at the same value of mass flow rate (0.86 and 82 kg/sec). At 100 percent of design speed the peak impeller efficiency occurs at a mass flow rate (0.98 kg/sec) that is lower than the mass flow rate (1.02 kg/sec) at which minimum diffuser total pressure loss occurs. At 80 and 100 percent design speed the mismatch in peak impeller efficiency and minimum diffuser total pressure loss appears to be the cause of the lower efficiency as compared to that for 90 percent design speed. Opening the inducer by 3 percent would shift all impeller curves to the right by 3 percent. This would make the peak impeller efficiency and the minimum diffuser total pressure loss occur at about the same

mass flow for 100 percent design speed and a maximum stage efficiency of about 0.796 would be expected at design speed with some decrease in the stage efficiency at the other speeds.

A design speed clearance setting of 6.4 percent was considered a reasonable operating clearance for a production machine since clearance at surge for this setting was very close to zero. Therefore, performance figures for the following discussion are for a 6.4 percent clearance. At design equivalent speed, peak efficiency was 0.778. Figure 12 is a cross plot of figure 10 and shows the variation of peak efficiency with clearance at design speed. Because the clearance was varied over such a small range, the actual shape of the efficiency versus clearance curve cannot be determined with accuracy. For the subject compressor this figure shows that peak efficiency is reduced as axial tip clearance is increased. The reduction is about 0.24 points for each 1 percent increase in axial clearance for clearances less than about 8.9 percent.

Figure 13 shows the variation of overall pressure ratio with equivalent mass flow and axial tip clearance. Surge is shown by the dashed line. For design speed, all four clearances are shown. For 80 percent speed and lower, pressure ratio changes only slightly and data is shown only at 6.4 percent clearance. At design speed, the peak pressure ratio was 6.13.

Figures 10 and 13 show that surge to choke flow range decreased from 16 to 6 percent of choked flow as equivalent speed was increased from 90 to 100 percent of design. Peak efficiency at 100 percent equivalent speed is about 1.1 points lower than at 90 percent. The reason for this drop in efficiency was discussed previously. At design speed, choking equivalent mass flow rate is 1.038 kilograms per second. This is about 1/2 percent above design flow rate. At design pressure ratio of 5.9 the flow rate is 1.015 kilograms per second which is about 1.8 percent below design flow rate. Differences between the actual impeller hardware and the design impeller were described under Deviations From Design and are probably responsible for lower than expected inducer choking flow.

When the mass flow-speed parameter at choke Ω_{choke} is plotted versus percent speed, the slope of the curve is positive for diffuser choke and negative for inducer choke. An explanation of the reason why this occurs is given in appendix B. Figure 14 indicates whether the vaned diffuser or the inducer is responsible for choking the stage. At about 95 percent speed, both vaned diffuser and inducer choke at the same mass flow as shown by the intersection of the two curves. At speeds above 95 percent, stage choke is controlled by the inducer. A plot with this parameter has been found to be a more accurate indicator of inducer-diffuser choke than temperature measurements.

Impeller Performance Obtained With Vaneless Diffuser

To determine the maximum flow range of the impeller, the original vane-island diffuser was replaced with a vaneless diffuser. Tests were made at axial tip clearances corresponding to 3.7, 5.7, 7.9, and 9.6 percent of blade height at design speed. The mass flow-speed parameter at choke, Ω_{choke}, is plotted versus percent speed in figure 14 and shows the same characteristic as for the vaned diffuser test. System choke occurs at speeds less than 92 percent. Inducer choke begins at 92 percent speed. All other results presented in this section are for design speed only.

Impeller performance. - Figures 15, 16, and 17 show impeller total efficiency, total pressure ratio, and work factor as functions of equivalent mass flow for four values of axial tip clearance. Impeller efficiency and pressure ratio were calculated using the method described in the section Procedure. The compressor was surged only with the 7.9 percent clearance. The surge to choke flow range was found to be 16.4 percent of choke flow as compared to 6 percent with the vaned diffuser. Figure 18 is a cross plot of figure 15 and shows peak impeller efficiency obtained with a vaneless diffuser as a function of clearance. Figure 18 shows that impeller peak efficiency increased roughly three points from 0.866 to 0.895 as the clearance was decreased from 9.6 to 3.7 percent. Thus, impeller peak efficiency improves about 0.5 points with each 1 percent decrease in clearance compared to 0.24 points for overall compressor efficiency with the vaned diffuser at 100 percent speed. Figure 16 shows that the pressure ratio increased with decreasing clearance at all flow rates. At an equivalent mass flow rate of 0.972 kilogram per second corresponding to surge with the vaned diffuser, the pressure ratio increased from 6.74 to 7.16. At the impeller design pressure ratio of 6.95 and a clearance of 3.7 percent the mass flow is 1.005 kilogram per second. This value is 3.4 percent from choke (1.04 kg/sec) and 2.7 percent from design flow (1.033 kg/sec). Impeller efficiency at 1.005 kilogram per second is 0.885 which is 0.014 points higher than the design value of 0.871. If the inducer blade normal thickness was reduced to design value (design area was reduced by 3 percent because of thicker than design inducer blades as mentioned previously under Compressor Design), the efficiency curve would be shifted about 3 percent toward higher flows. The impeller only efficiency at design flow would be about 0.885. To obtain peak impeller efficiency at design flow rate the inducer would have to be opened up about 8 percent. Figure 17 shows that impeller work was only slightly affected by clearance changes. The overall spread in work factor was less than 0.01 over the entire clearance range. Work factor showed a very slight apparent decrease of about 0.003 as the clearance was decreased from 9.6 to 7.9 percent but increased with further reductions in clearance. This was not considered significant since a 0.2 percent error in speed would change the work factor by 0.003.

Recirculation losses. - Figure 19 shows the comparison between design speed impeller efficiencies obtained with the vane-island diffuser and with the vaneless diffuser at an equivalent mass flow of 0.98 kilogram per second. This value of mass flow is close to surge with the vane-island diffuser. Efficiencies from the tests with the vaneless diffuser are about two points higher than those from the vane-island diffuser tests. This two point difference is usually attributed to the recirculation between the impeller and diffuser which was mentioned previously. Using the method of reference 2, a recirculation loss of 2.5 points was calculated at this flow. This indicates good agreement between the calculated and experimental values of recirculation loss.

Impeller-Diffuser Match

The matching characteristics of the impeller and diffuser is graphically shown in figure 20 as a function of speed for a 3.9 percent clearance at design speed. In this figure mass flow-speed parameter Ω for peak impeller efficiency from the vaneless diffuser, inducer choke with the vaneless diffuser, stage surge with the vaned diffuser and peak pressure recovery coefficient of the vaned diffuser are shown as functions of percent equivalent speed. This figure shows that peak impeller efficiency occurs at mass flows which are much higher than the mass flow for both peak diffuser recovery and diffuser choke at 50, 60, and 70 percent speeds. At 76.5, 92, and 99 percent speeds the impeller peak efficiency curve intersects with the diffuser choke line, the peak diffuser pressure recovery line and the stage surge line, respectively. Since peak impeller efficiency and minimum diffuser total pressure loss (fig. 11) are about the same levels for 80, 90, and 100 percent speeds, peak stage efficiency with the vaned diffuser should occur at the intersection of the peak impeller efficiency line and the peak diffuser pressure recovery line which for this configuration occurred at 92 percent speed. No data were taken at 92 percent speed but the peak efficiency attainable with this configuration should be close to that obtained at 90 percent speed since the match there was very good. Figure 20 also shows that the mismatch in mass flow rate at peak impeller efficiency and peak diffuser pressure recovery is greater at 80 percent speed than at 100 percent speed. Since the decrease in stage efficiency from 90 to 80 percent is slightly less than the decrease in stage efficiency from 90 percent speed to 100 percent speed, it can be concluded that mismatches where the peak impeller efficiency is on the choke side of peak diffuser pressure recovery is less severe than when the impeller peak efficiency is on the surge side of peak diffuser pressure recovery. This results from the fact that there is a very sharp drop in impeller efficiency as the impeller goes into choke whereas there is a more gradual drop in efficiency as the mass flow is reduced toward surge.

A rematch of the diffuser-impeller area can be expected to give a design speed stage efficiency near or somewhat exceeding the 0.796 obtained at 90 percent speed, if it can

be assumed that the diffuser peak recovery does not change its position with respect to the diffuser choke line and the level of peak pressure recovery does not change with small changes in diffuser setting angle. Reducing the diffuser throat area about 6 percent by rotating the diffuser vanes toward tangential by about 2° should match up the diffuser and impeller to give a peak efficiency near 0.80 at design speed with a small penalty in efficiency at lower speeds. If the aforementioned assumptions are true, a decrease in surge mass flow of about 6 percent can also be expected.

CONCLUDING REMARKS

Tests of the vaned diffuser and vaneless diffuser with the impeller have indicated potential for improving peak stage efficiency to about 0.80 at design speed and 3.9 percent clearance. This could be accomplished by increasing the inducer area or reducing diffuser area to provide a better match of impeller and diffuser characteristics at 100 percent speed. Rotation of the diffuser vanes toward tangential would provide the desired area reduction and possibly decrease surge mass flow rate by providing better incidence at the diffuser leading edge.

SUMMARY OF RESULTS

The performance of a centrifugal compressor was investigated. The impeller had a 16.10 centimeter tip diameter and backswept blading. Inspection of the impeller showed the following:

1. Thickness at the tip is nearly twice the design value.
2. Blade angle β_b at the exit is 2° to 3.5° lower than design.
3. Thickness at the exit is about twice the design value.

For design point operation in air, the compressor design total pressure ratio is 5.9:1 at an equivalent mass flow rate of 1.033 kilograms per second. After determining the overall performance, the vane-island diffuser was replaced by a vaneless diffuser to determine impeller performance. The following results were obtained from overall performance tests:

1. Peak overall efficiency at design aerodynamic speed and 6.4 percent hot axial tip clearance was 0.778. Peak total pressure ratio was 6.13.

2. Maximum overall efficiency at 3.9 percent design speed clearance was 0.796 at 90 percent speed where impeller and diffuser characteristics were best matched.

3. A large decrease in operating range occurred when speed was increased from 90 to 100 percent of design. Based on choking flow rate, at a hot axial tip clearance of 6.4 percent, the range between choke and surge decreased from 16 to 6 percent.

4. Equivalent mass flow rate at design speed and pressure ratio with a hot axial tip clearance of 6.4 percent is 1.8 percent less than design. The actual choking equivalent mass flow rate at design aerodynamic speed is very close to the design operating value of 1.033 kilograms per second.

5. At equivalent speeds above 95 percent, choking flow rate is governed by inducer choke. At lower speeds, choking flow rate is determined by diffuser choke.

The following results were obtained for design equivalent speed from impeller tests in which the vane-island diffuser was replaced by a vaneless diffuser.

1. Peak impeller efficiency at design speed increased from 0.866 to 0.895 as axial tip clearance was decreased from 9.6 to 3.7 percent.

2. Peak impeller efficiency occurred at a mass flow less than the surge flow with the vaned diffuser.

3. Pressure ratio always increased as the clearance was decreased from 9.6 to 3.7 percent. At an equivalent mass flow rate of 0.972 kilogram per second, the impeller pressure ratio increased from 6.74 to 7.16.

4. Impeller surge to choke flow range was 16 percent of choke flow.

Lewis Research Center,
National Aeronautics and Space Administration,
and
U.S. Army Air Mobility R&D Laboratory,
Cleveland, Ohio, April 1, 1977,
505-04.

APPENDIX A

SYMBOLS

A	area, m^2
a	speed of sound, m/sec
CP	diffuser pressure recovery, $(p_3 - p_2)/(p_2' - p_2)$
c_p	specific heat at constant pressure, J/(kg)(K)
$\Delta h'$	specific work, J/kg
K	constant
N	rotative speed, rpm
N_s	specific speed, dimensionless
p	pressure, N/m^2
Q	volume flow rate, m^3/sec
R	gas constant, J/(kg)(K)
T	temperature, K
U	blade speed, m/sec
V	absolute gas velocity, m/sec
W	relative gas velocity, m/sec
w	mass flow rate, kg/sec
α	absolute flow angle, deg from meridional plane
β	relative flow angle, deg from meridional plane
β_b	angle of blade mean camber line to meridional plane, deg
γ	ratio of specific heats
Δ	change in clearance, percent of blade height at exit
δ	ratio of inlet total pressure to U.S. standard sea-level pressure, p'/p^*
η	compressor adiabatic temperature rise efficiency, $\frac{\text{ideal total enthalpy rise}}{\text{actual total enthalpy rise}}$
Θ	ratio of compressor inlet total temperature to U.S. standard sea-level temperature, T'/T^*
ρ	gas density, kg/m^3

Ω mass flow-speed parameter, $\left[(w/N)/(w/N)_{design}\right]^*$

ω impeller angular velocity, rad/sec

$\overline{\omega}$ diffuser total pressure loss coefficient, $(p'_2 - p'_3)/(p'_2 - p_2)$

Subscripts:

choke compressor operating at choking mass flow rate

cr condition corresponding to Mach number of unity

D station at diffuser throat

id ideal

m meridional component

u tangential component

0 station at bellmouth inlet

1 inducer inlet (fig. 8)

2 impeller exit (fig. 8)

3 exit of vaneless space downstream from vaned diffuser (fig. 8)

Superscripts:

' absolute total state

* U.S. standard sea-level conditions (temperature, 288.15 K; pressure, 10.13 N/cm^2 abs)

APPENDIX B

THEORETICAL VARIATION OF DIFFUSER AND INDUCER CHOKING MASS FLOW RATES WITH EQUIVALENT SPEED

If the quantity $\left(w\sqrt{\theta}/\delta\right)\Big/\left(U_2/\sqrt{\theta}\right)$ for choked flow is plotted as the ordinate against $U_2/\sqrt{\theta}$, the slope will generally be positive for diffuser controlled flow and will always be negative for inducer controlled flow. The equivalent speed at which the slope changes sign is the minimum speed for inducer control of the choking flow rate. This method of determining the speed ranges for inducer and diffuser choke is more reliable than estimates obtained from temperature rise data.

A simple one-dimensional flow analysis will be used to explain why the slope is positive for diffuser control and negative for inducer control. Blade loading and hub-to-tip flow variations will be ignored. The working fluid is assumed to be a perfect gas undergoing an isentropic process. Therefore, the ratio of specific heats γ and the heat capacity c_p are constants.

Diffuser Controlled Flow

Three additional assumptions are made for diffuser controlled flow:

(1) Constant values of absolute flow angle α_2 and relative flow angle β_2 at the impeller tip

(2) Constant value of absolute flow angle α_D at the diffuser throat

(3) Zero prewhirl at the impeller inlet

From the first assumption

$$V_{u,2} = KU_2 \tag{B1}$$

The constant K depends on α_2 and β_2. From the second assumption, we can define a constant geometrical diffuser throat area A_D normal to the flow. The continuity equation applied to condition at the diffuser throat can be written as

$$w = \left(\frac{\rho}{\rho'}\right)_D \left(\frac{V}{V_{cr}}\right)_D \rho_2' V_{cr,2} A_D \tag{B2}$$

For choking flow $\left(V/V_{cr}\right)_D = 1$ and

$$\left(\frac{\rho}{\rho'}\right)_D \left(\frac{V}{V_{cr}}\right)_D = \left(\frac{2}{\gamma + 1}\right)^{1/(\gamma-1)} \tag{B3}$$

The perfect gas law, energy equation, and equation (B1) can be combined to obtain

$$\rho_2' = \frac{p_1'}{RT_1'}\left(\frac{KU_2^2}{c_p T_1'} + 1\right)^{1/(\gamma-1)} \tag{B4}$$

and

$$V_{cr,2} = \sqrt{\left(\frac{2\gamma}{\gamma + 1}\right) RT_1' \left(\frac{KU_2^2}{c_p T_1'} + 1\right)} \tag{B5}$$

When equation (B2) is divided by $U_2/\sqrt{\theta}$, and equations (B3), (B4), and (B5) are substituted into equation (B2),

$$\frac{\frac{w\sqrt{\theta}}{\delta}}{\frac{U_2}{\sqrt{\theta}}} = \frac{\rho^* a^* A_D \left\{\left(\frac{2}{\gamma + 1}\right)\left[\frac{K}{c_p T^*}\left(\frac{U_2}{\sqrt{\theta}}\right)^2 + 1\right]\right\}^{\gamma+1/2(\gamma-1)}}{\frac{U_2}{\sqrt{\theta}}} \tag{B6}$$

where

$$\rho^* = \frac{p^*}{RT^*} \quad \text{and} \quad a^* = \sqrt{\gamma RT^*}$$

For realistic values of gas properties, the slope of the $\left(w\sqrt{\theta}/\delta\right)/\left(U_2/\sqrt{\theta}\right)$ versus $U_2/\sqrt{\theta}$ curve is negative for low values of $U_2/\sqrt{\theta}$. The curve has a minimum point. When $d\left[\left(w\sqrt{\theta}/\delta\right)/\left(U_2/\sqrt{\theta}\right)\right]/d\left(U_2/\sqrt{\theta}\right) = 0$,

$$\frac{U_2}{\sqrt{\theta}} = \frac{a^*}{\sqrt{2K}} \tag{B7}$$

Above this speed, the slope is positive. The subject compressor has a K value of approximately 0.75 at the design point. The design value of $U_2/\sqrt{\theta}$ is 576 m/s. The minimum point should be at about 48 percent of design equivalent speed for this machine.

From figure 20, the minimum point determined experimentally is at about 53 percent speed.

Inducer Controlled Flow

Two additional assumptions are made for inducer controlled flow:

(1) Constant relative inlet flow angle

(2) Zero prewhirl at the impeller inlet

From these assumptions,

$$V_1 = \frac{U_1}{\tan \beta_1} \tag{B8}$$

The mass flow rate w is obtained from continuity; thus,

$$w = \left(\frac{\rho}{\rho'}\right)_1 \rho_1' V_1 A_{m,1} \tag{B9}$$

The area $A_{m,1}$ is the inducer inlet area normal to the meridional flow. From equation (B8), the velocity ratio V/V_{cr} can be expressed as

$$\left(\frac{V}{V_{cr}}\right)_1 = \frac{U_1}{\tan \beta_1 \sqrt{\left(\frac{2\gamma}{\gamma + 1}\right) RT_1'}} \tag{B10}$$

Since

$$V_{cr,1} = \sqrt{\frac{2\gamma}{\gamma + 1} RT_1'}$$

From equation (B10) the density ratio ρ/ρ', is expressed as

$$\left(\frac{\rho}{\rho'}\right)_1 = \left[1 - \left(\frac{\gamma - 1}{2\gamma}\right) \frac{U_1^2}{RT_1' \tan^2 \beta_1}\right]^{1/(\gamma-1)} \tag{B11}$$

When equations (B8), (B11), and the perfect gas law are substituted into equation (B9) and the result is divided by U_1,

$$\frac{\frac{w\sqrt{\theta}}{\delta}}{\frac{U_1}{\sqrt{\theta}}} = \frac{\rho^* A_{m,1}}{\tan \beta_1} \left[1 - \left(\frac{\gamma - 1}{2\gamma} \right) \frac{\left(\frac{U_1}{\sqrt{\theta}} \right)^2}{RT^* \tan^2 \beta_1} \right]^{1/(\gamma-1)} \tag{B12}$$

Obviously the value will decrease as $U_1/\sqrt{\theta}$ increases. Since the ratio U_2/U_1 is a constant, the slope of the $\left(w\sqrt{\theta}/\delta\right)\Big/U_2/\sqrt{\theta}$ plotted against $U_2/\sqrt{\theta}$ curve will be negative.

REFERENCES

1. Perrone, G. L.; Holbrook, M. R.; and McVaugh, J. M.: Backswept Impeller and Vane-Island Diffuser and Shroud for NASA Advanced-Concepts Compressor Test Rig. (AT-6131-R, AiResearch Mfg. Co.; NAS3-15328), NASA CR-120942, 1973.
2. Galvas, Michael R.: Analytical Correlation of Centrifugal Compressor Design Geometry for Maximum Efficiency with Specific Speed. NASA TN D-6724, 1972.

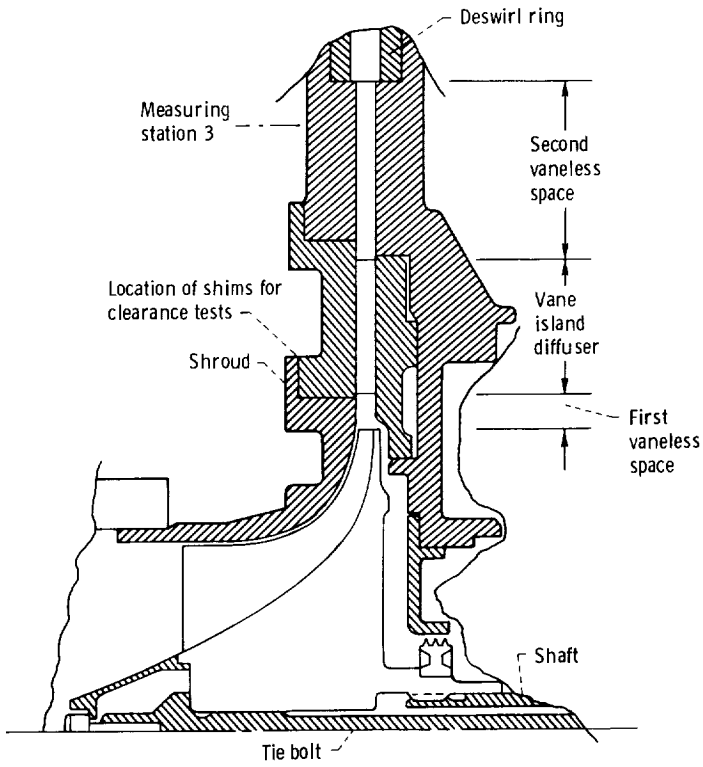

Figure 1. - Meridional view of compressor.

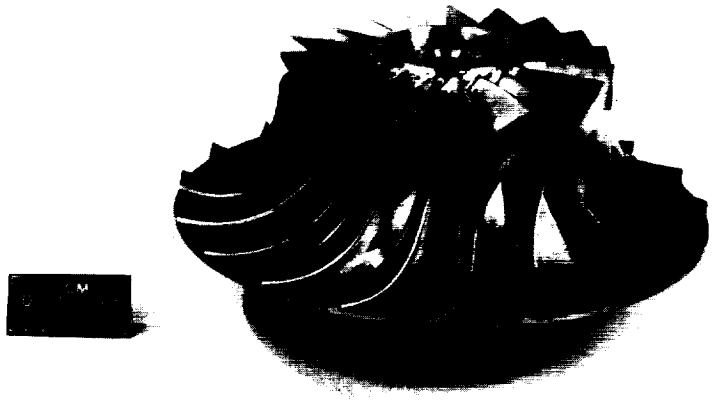

Figure 2. - Impeller.

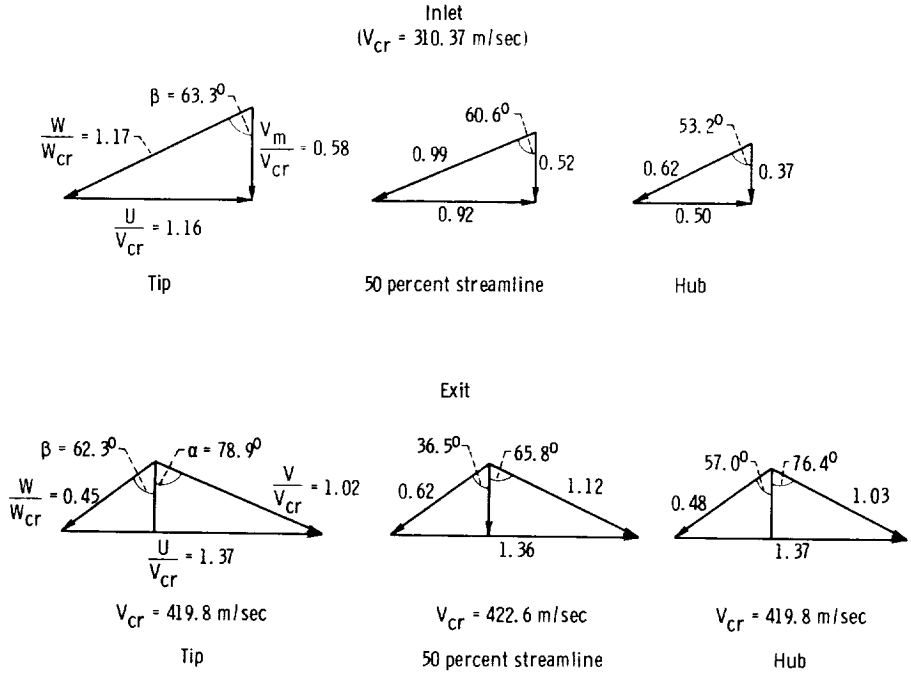

Figure 3. - Design impeller velocity diagrams; inside blade.

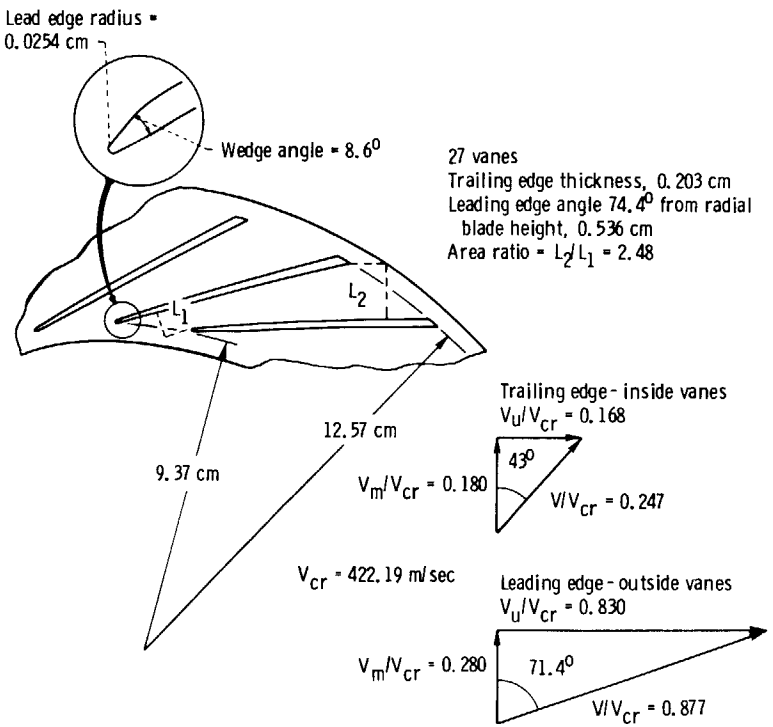

Figure 4. - Diffuser vanes and design velocity diagrams.

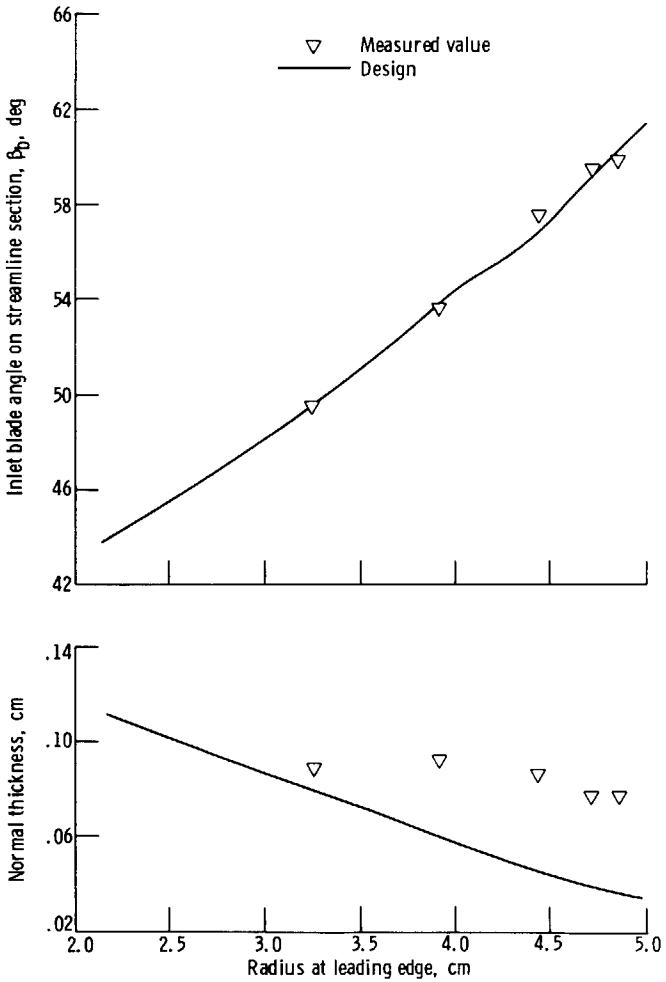

Figure 5. - Comparison of design and measured impeller leading edge geometry.

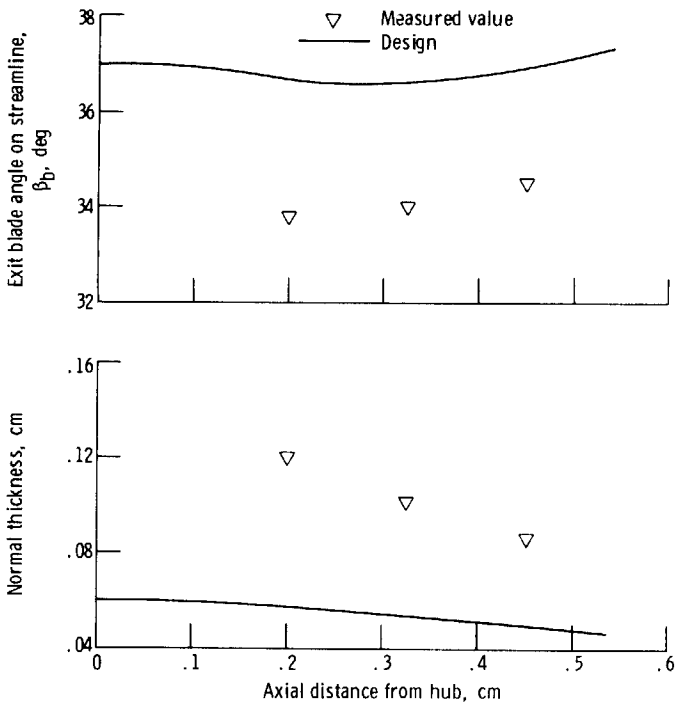

Figure 6. - Comparison of design and measured impeller exit geometry.

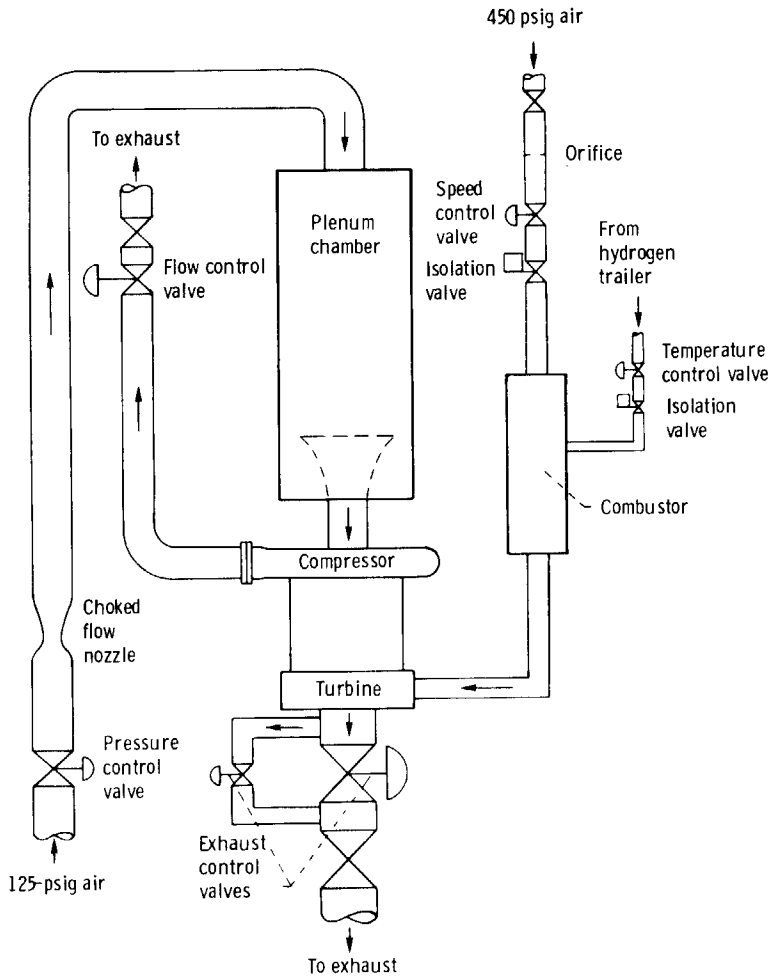

Figure 7. - Test facility schematic.

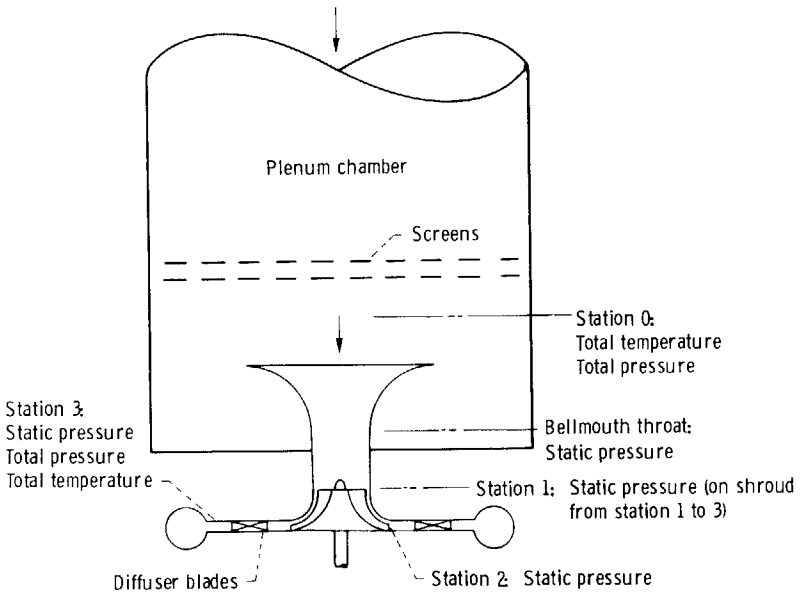

Figure 8. - Inlet, exit, and bellmouth measuring stations.

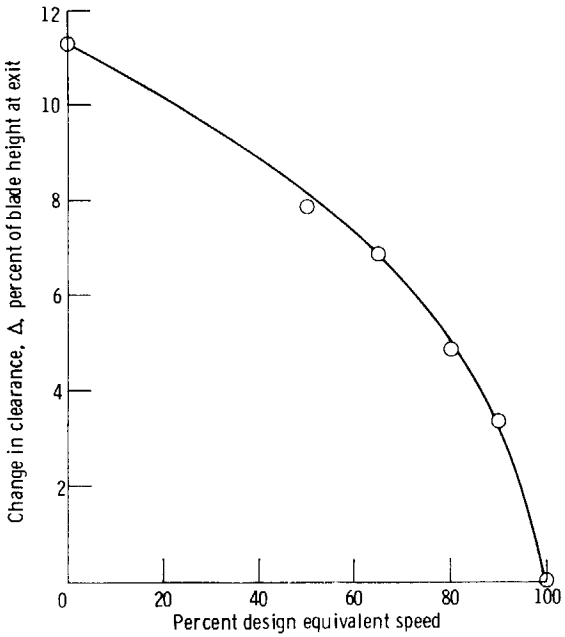

Figure 9. - Change in percent clearance as function of equivalent speed. Percent clearance equals percent clearance at design equivalent speed + Δ.

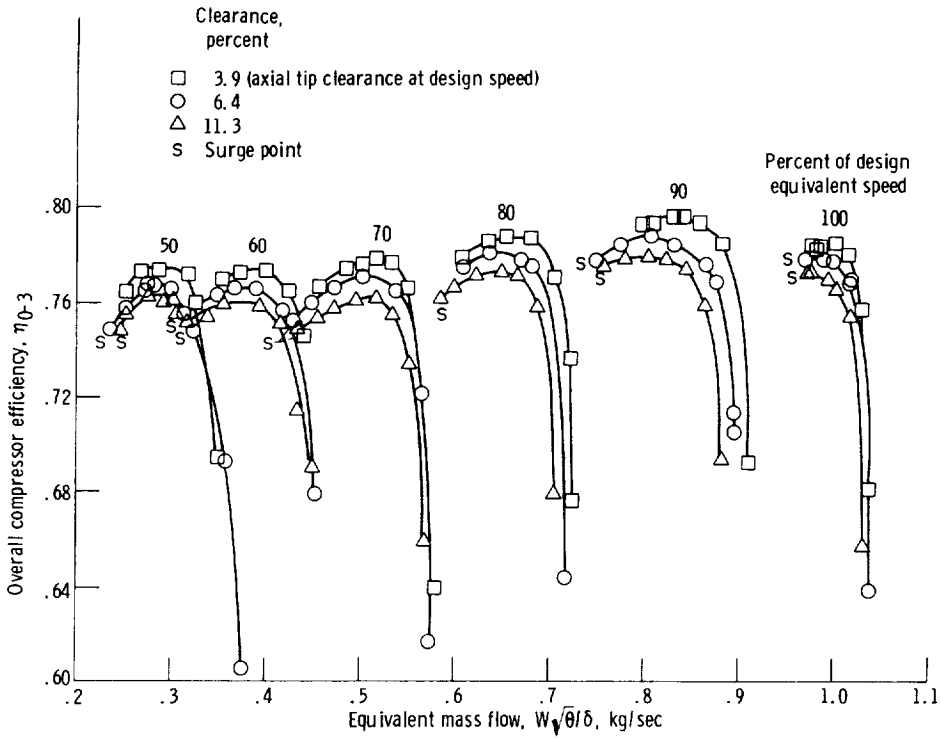

Figure 10. - Variation of total efficiency with equivalent mass flow, equivalent speed, and axial tip clearance; vaned diffuser test.

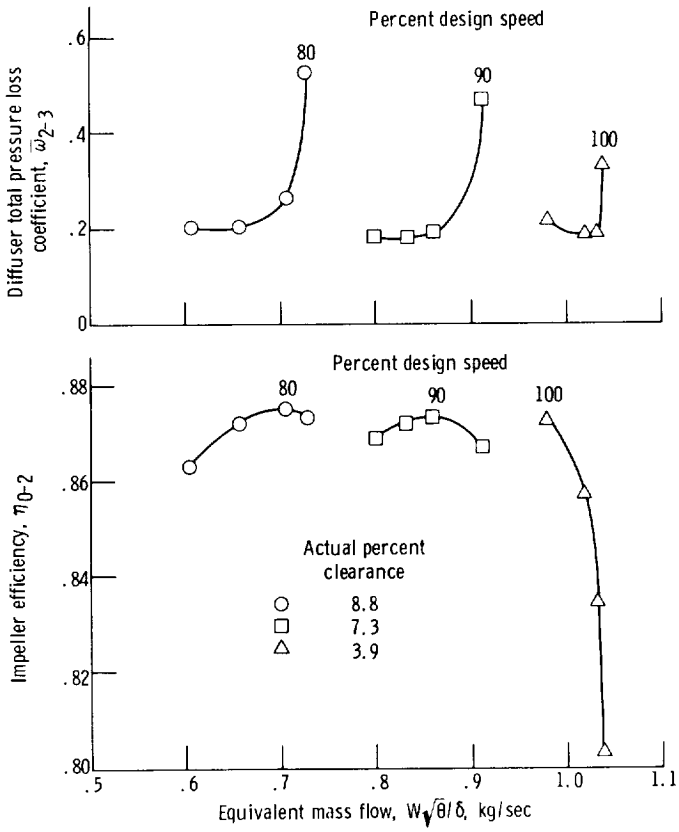

Figure 11. - Overall diffuser total pressure loss and impeller efficiency versus mass flow; vaned diffuser tests. Ratio of specific heats $\gamma = 1.4$.

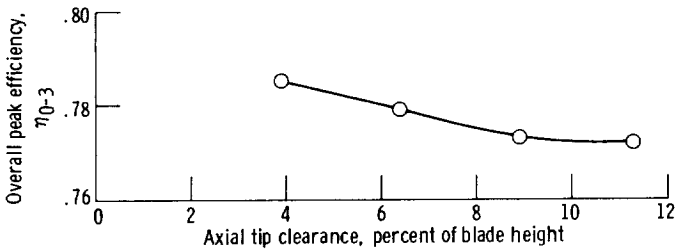

Figure 12. - Variation of overall peak efficiency with axial tip clearance; design equivalent speed; vaned diffuser tests.

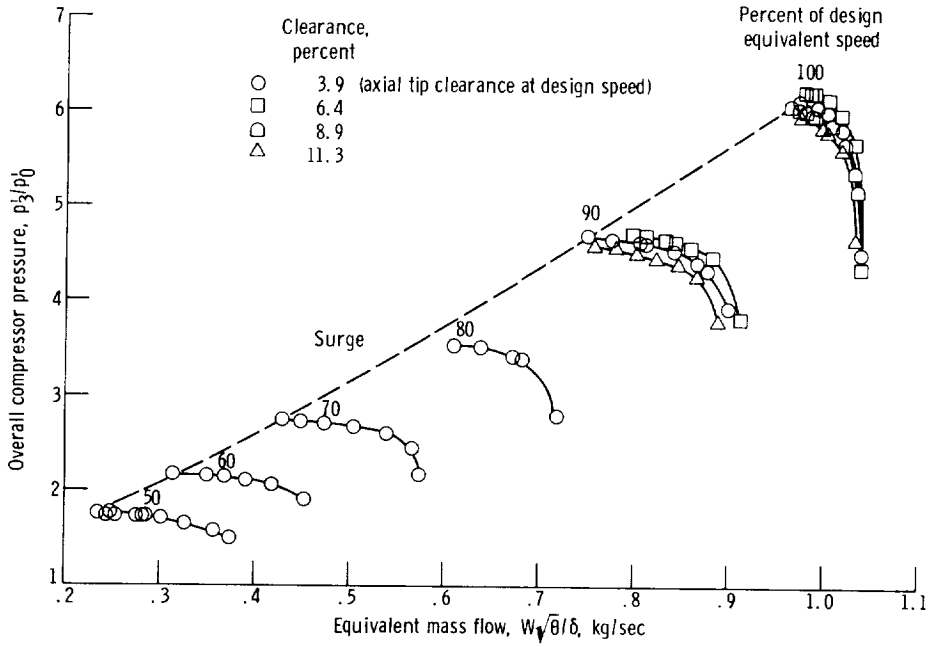

Figure 13. - Variation of total pressure ratio with equivalent mass flow, equivalent speed, and axial tip clearance; vaned diffuser test.

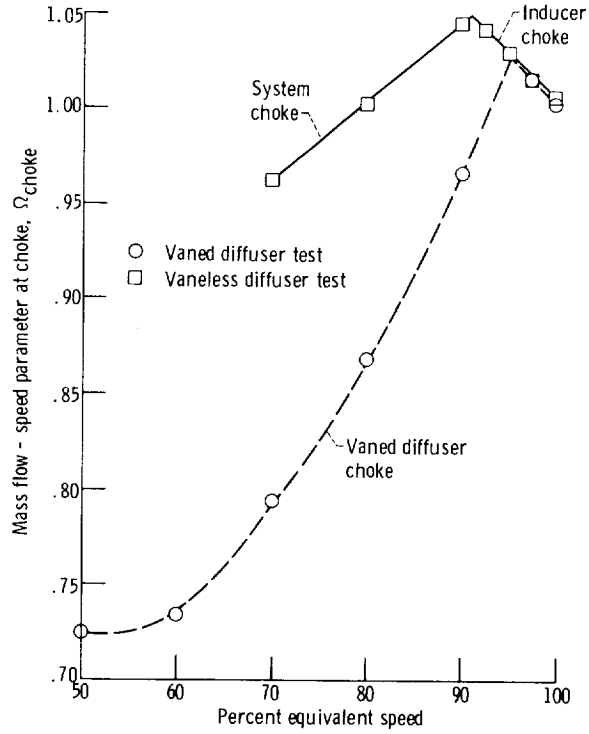

Figure 14. - Determination of equivalent speed at which inducer chokes.

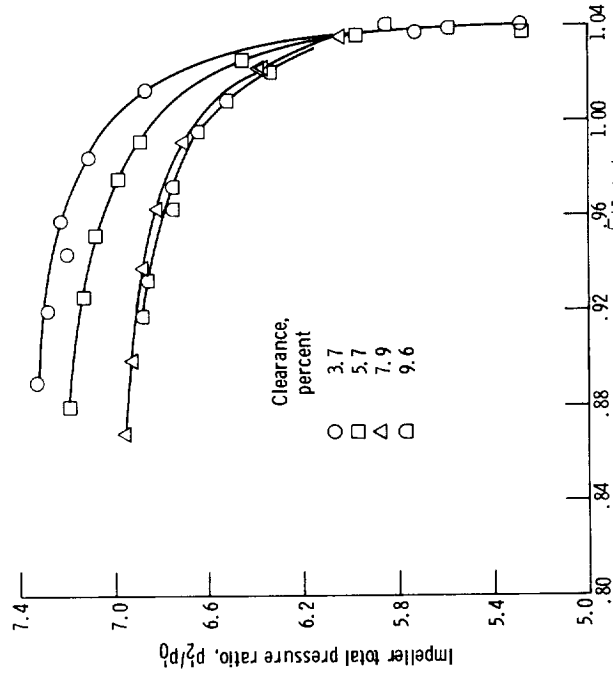

Figure 16. - Variation of impeller total pressure ratio with flow rate and clearance; design speed; vaneless diffuser test. Ratio of specific heat, $\gamma = 1.4$.

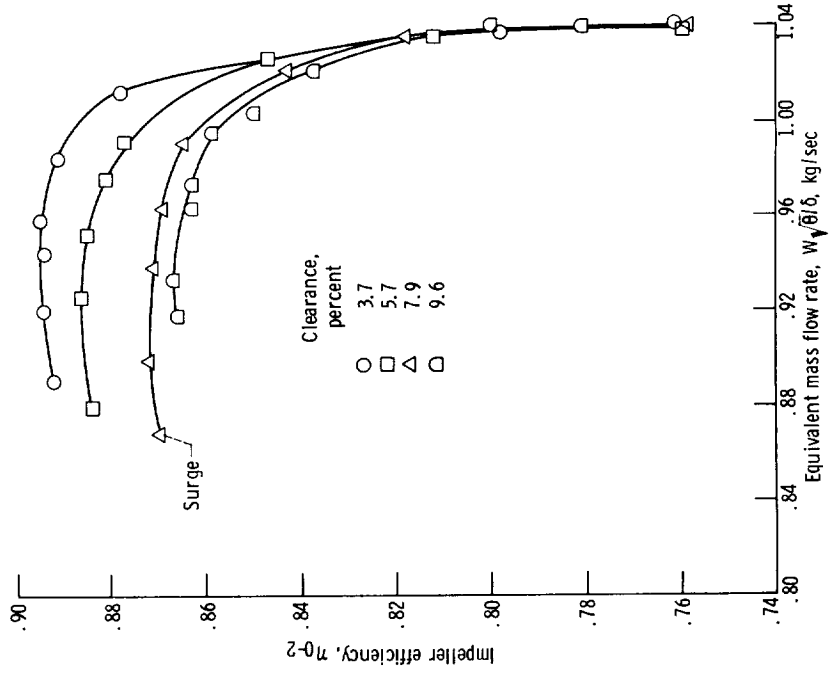

Figure 15. - Variation of impeller efficiency with flow rate and clearance; design speed; vaneless diffuser test. Ratio of specific heat $\gamma = 1.4$.

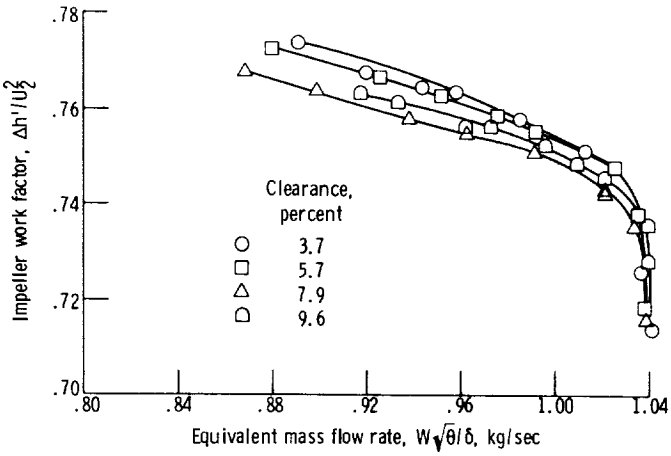

Figure 17. - Variation of impeller work factor with flow rate and clearance; design speed; vaneless diffuser test. Ratio of specific heat $\gamma = 1.4$.

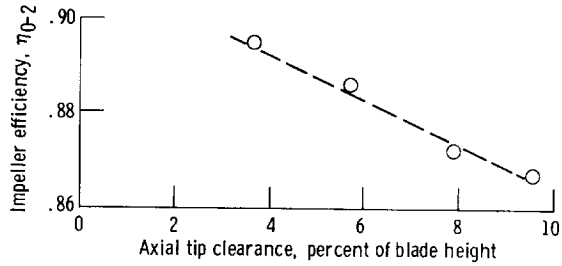

Figure 18. - Variation of impeller peak efficiency with axial tip clearance for vaneless diffuser test. Ratio of specific heat $\gamma = 1.4$.

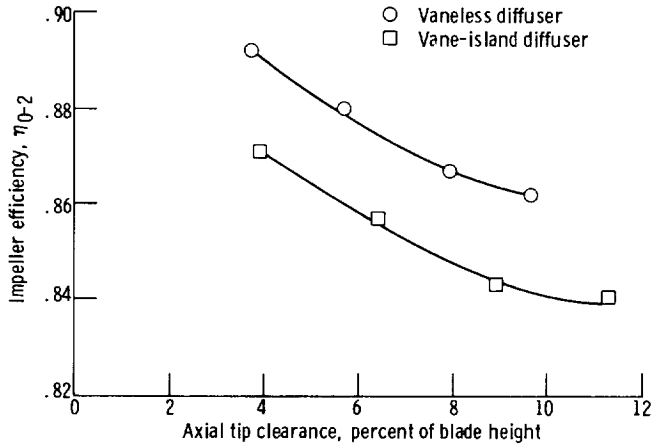

Figure 19. - Variation of impeller efficiency with axial tip clearance. Equivalent mass flow $W\sqrt{\theta}/\delta = 0.98$ kg/sec; ratio of specific heats $\gamma = 1.4$.

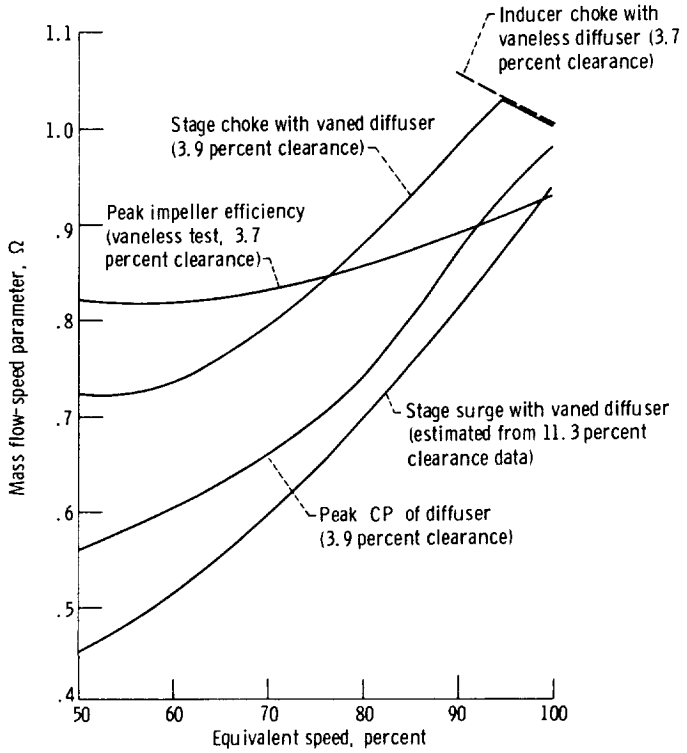

Figure 20. - Mass flow-speed parameter versus percent equivalent speed showing relationship of impeller/diffuser characteristics.